# Monte Carlo study of low and high-field electron transport in GaN-based heterostructures

J.-L. Thobel, F. Dessenne, and C. Dalle
Institut d'Electronique, de Microélectronique et de Nanotechnologies, UMR CNRS 8520, Université Lille1, Avenue Poincaré 59652 Villeneuve d'Ascq Cédex, France
e-mail: Jean-Luc.Thobel@iemn.univ-lille1.fr

## INTRODUCTION

GaN-based heterostructures have proven to be extremely useful for the realization of high speed, high power HEMTs devices. Using $Al_{1-x}In_xN$ barrier, instead of the more common AlGaN material, allows to achieve higher electron densities $N_S$. Moreover, when x≅0.18, this material is lattice-matched to GaN, thus avoiding strain related issues. In the existing literature there are a few reports of Monte Carlo simulation of 2D electron transport in GaN-based heterostructures, but most of them are limited to the mobility regime and to $N_S \leq 2 \times 10^{13}$ cm$^{-2}$. To overcome these limitations, in the present work, we consider size quantization in all valleys, with a large number of subbands and we properly account for the strong degeneracy of the electron gas.

## MODEL

Schrödinger/Poisson equations are solved and the electron states used to compute the scattering rates. In many circumstances, a large number of subbands contribute to the transport: at high driving electric fields, because electron distribution is spread over a wide range of energy; at low $N_S$, whatever the field intensity, because subbands are closely spaced. We take up to 100 subbands and consider that electron states related to satellite valleys are also quantized. This approach allows us to describe electron transport in a wide range of field without resorting to the awkward concept of '2D-3D transfers'.

Owing to the very high electron densities that may be reached, it is essential to properly account for degeneracy. We have included the Pauli principle using the method described in [1].

The following scattering mechanisms are accounted for: phonons (polar optic, acoustic and intervalley), alloy, ionized impurities and threading dislocations. In principle, dynamical screening should be considered for the inelastic phonon scattering. In many-subband systems this is an unmanageable task and in most studies LO phonon scattering is simply left unscreened. However, for GaN-based-heterostructures, this gives calculated mobilities below the measured ones. Therefore, we choose to apply static screening to all scattering mechanisms, as proposed by Polyakov et al. [2].

Material parameters relative to the lowest valley are summarized in table I. Parameters relative to upper valleys are poorly known and the published values are widely scattered [3]. We consider spherical nonparabolic valleys U and $\Gamma_3$ located respectively 1.9 and 2.5 eV above the minimum of conduction band in GaN.

## RESULTS

Fig. 1 and 2 show typical structures, $N_S$-$V_G$ characteristics, and computed wavefunctions. In the following, we consider 10 nm AlInN barrier. The mobility $\mu$ is shown as a function of $N_S$ in fig. 3. When dislocation density is negligible, $\mu$ presents a maximum at $N_S \cong 2.5 \times 10^{12}$ cm$^{-2}$. At lower Ns, $\mu$ is reduced due to intersubband scattering, whereas for higher Ns, $\mu$ is negatively affected by the enhancement of phonon emission due to increased energy. This effect is directly related to degeneracy. When dislocation scattering dominates, $\mu$ is strongly reduced at low $N_S$ and increases monotonically with Ns.

Thanks to the large number of subbands, fields as high as 300kV/cm can be considered. Velocity-field characteristics are shown in fig. 4 for several values of $N_S$. Peak velocity is slightly above $3\times10^7$cm/s at low $N_S$. Remarkably, when $N_S$ is increased, peak velocity and critical field are reduced. The reason is that intervalley transfers require less energy, owing to degeneracy and confinement.

ISBN 978-2-9547858-0-6

## Acknowledgment

This work has been supported by the French Agence Nationale de la Recherche (ANR) under reference ANR-11-INFR-0002.


## References


[1] P. Borowik and J.-L. Thobel, *Improved Monte Carlo method for the study of electron transport in degenerate semiconductors*, J. Appl. Phys. **84**(7), pp. 3706-3709 (1998)

[2} V. M. Polyakov, F. Schwierz, I. Cimalla, M. Kittler, B. Lübbers and A. Schober, *Intrinsically limited mobility of the two-dimensional electron gas in gated AlGaN/GaN and AlGaN/AlN/GaN heterostructures,* J. Appl. Phys. **106**, 023715 (2009)

[3] V. Palankovski, A. Marchlewski, E. Ungersbock, and S. Selberherr, *Identification of transport parameters for Gallium nitride based semiconductor devices*, Proc. 5th MATHMOD, Vienna, pp. 14-1-9 (2006)


| Parameter | GaN | AlN | $AlIn_{0.18}N$ |
|---|---|---|---|
| Mass $m_\Gamma$* | 0.19 | 0.27 | 0.24 |
| Nonparabolicity $\alpha(eV^{-1})$ | 0.19 | 0.09 | 0.12 |
| Acoustic. Def. Pot. $\Phi_a$ (eV) | 8.3 | 9.5 | 9 |
| Static permittivity | 9.5 | 8.5 | 9.72 |
| H.F. permittivity | 5.35 | 4.77 | 5.43 |
| LO phonon (meV) | 92 | 100 | 95 |

Table 1. Material parameters relative to $\Gamma_3$ valley.
Other important parameters are the mass of upper valleys U and $\Gamma_3$, taken equal to 0.6, and the band offsets: 1.9 eV between GaN and AlN and 1. eV between AlN and AlInN.

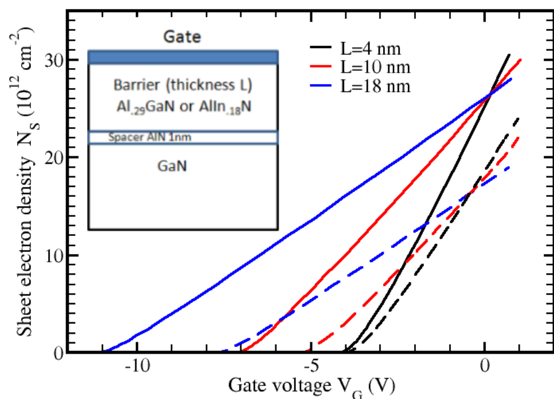


Figure 1. Charge control characteristics $N_S(V_G)$. The Considered structures are sketched in the insert: the gate is deposited on the barrier (made of $Al_{0.82}In_{0.18}N$ or $Al_{0.29}Ga_{0.71}N$). The GaN is separated from the barrier by a 1 nm AlN spacer layer. $V_G$ is the 'internal gate voltage' which includes Schottky barrier. Solid lines are for $Al_{0.82}In_{0.18}N$ barrier, dashed lines for $Al_{0.29}Ga_{0.71}N$ barriers

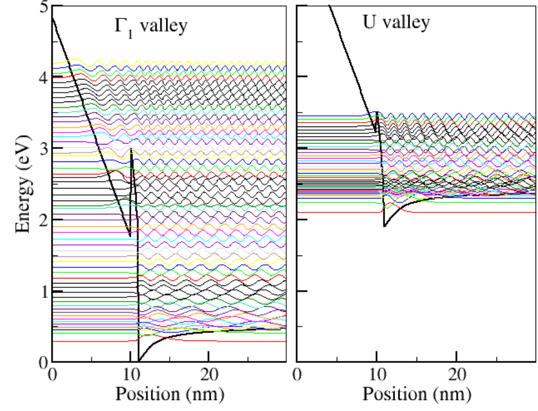


Figure 2. Band profile and first 60 wavefunctions in the two lowest valleys, obtained by self-consistent Schrödinger/Poisson resolution for $N_S = 10^{13}$ cm$^{-2}$. The depth of the GaN layer has been taken equal to 28 nm

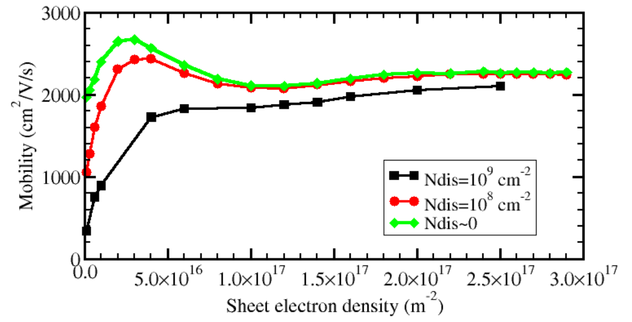


Figure 3. Low-field mobility as a function of the sheet carrier density $N_S$ for several values of dislocation density. (room temperature, structure with 10nm AlInN)

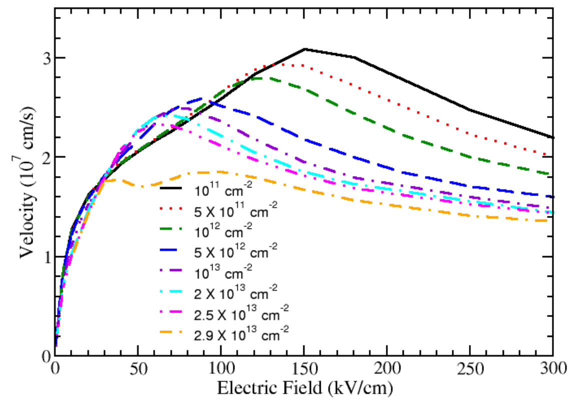


Figure 4. Velocity-Field characteristics for several values of the sheet carrier density $N_S$ ( room temperature, structure with 10 nm AlInN, negligible dislocation density)